ARCHIVES
of
FOUNDRY ENGINEERING

ISSN (2299-2944)
Volume 2026
Issue 1/2026

147 – 156

18/1

10.24425/afe.2026.157981

Published quarterly as the organ of the Foundry Commission of the Polish Academy of Sciences

Influence of Thermal Conditions During Plaster-based Investment Flask Casting on the Properties of AlSi10Mg Alloy

K. Miczková *, P. Lichý
VSB - Technical University of Ostrava, Czech Republic
* Corresponding author: E-mail address: katerina.miczkova@vsb.cz

Received 30.09.2025; accepted in revised form 29.12.2025; available online 30.03.2026

Abstract

This study examines the influence of plaster-based flask mould cooling conditions on the as cast structure and properties of AlSi10Mg alloy. The aim was to describe how different combinations of pouring and mould temperatures affect the alloy's behaviour during solidification. While the effect of pouring temperature on casting properties is well known, this study extends the analysis to explore the impact of mould preheating, providing a broader understanding of how cooling rates influence microstructure, fluidity, linear thermal expansion, and mechanical properties such as tensile and compressive strength. These parameters were assessed under different casting conditions.
Microstructure analysis combined optical observation and quantitative SDAS measurement. The results confirmed that lower mould temperatures (25 °C) produced finer-grained structures with fewer shrinkage cavities and porosities, resulting in higher mechanical properties. However, these conditions reduced fluidity and increased thermal expansion. In contrast, moulds preheated to 580 °C improved fluidity and reduced thermal expansion but led to coarser microstructures and lower mechanical properties.
The study identified the optimal casting conditions for balancing fluidity, mechanical properties, and thermal stability. Lower mould temperatures (25 °C) combined with higher pouring temperatures (680 °C or 730 °C) helped offset the reduced fluidity caused by rapid cooling, while still maintaining acceptable mechanical properties and relatively low thermal expansion. The results also showed that using extremely high mould temperatures significantly reduces mechanical performance. For practical applications, preheating moulds to more moderate temperatures would provide a better balance across all measured properties. Future research could further refine these temperature ranges to optimize process parameters for geometrically complex and thin-walled castings, as well as other demanding applications.

Keywords: Aluminium alloys, Plaster flask mould temperature, Castability, Linear thermal dilatation, Microstructure

1. Introduction

In modern manufacturing, obtaining high-quality materials has become an essential requirement across most industrial sectors. With the rapid expansion of the automotive and aerospace industries, the demand for highly durable, reliable, and lightweight materials has become a top priority. This has driven the increasing use of metal alloys in recent years, as they offer superior mechanical properties that can be adjusted by modifying the composition of alloying elements to meet specific application requirements. Additionally, alloys provide the advantage of achieving the desired material properties while maintaining cost efficiency in terms of raw material supply and production. [1]

A key advantage of modern metallurgy is the advanced testing methods available to evaluate material performance. In the automotive industry, for example, rigorous quality control is one of the most critical factors. Since these materials are used in

the manufacture of critical machine components, ensuring long-term operational reliability and preventing failures that could lead to accidents due to material defects is essential. As a result, the highest priority in foundry and metal processing operations is placed on achieving 100% material quality through state-of-the-art inspection and testing techniques. [1][2]

Among the materials that meet the demands for low weight and high strength, aluminium alloys stand out. While pure aluminium had been industrially produced since the 19th century, its application as a structural material was initially limited. Significant progress occurred in 1906 with the development of an aluminium alloy commonly known as duralumin. It was discovered that the addition of alloying elements such as copper and magnesium significantly enhanced the mechanical properties of the resulting alloy compared to pure aluminium. This breakthrough was widely adopted in the automotive sector, and the trend continues to this day. [3][4]

Aluminium alloys are now commonly used in the production of engine blocks, chassis frames, radiators, pumps, high quality cast wheels, and other essential components, contributing to reduced vehicle weight and improved overall performance. [5][6][7]

1.1. Casting of Non-Ferrous Metals and Material Testing

The primary goal in non-ferrous metal casting is to achieve high-quality molten metal while minimizing energy consumption and overall melting costs. The most critical factors influencing the quality of the final alloy include charge materials, the type of melting furnace, the type of holding furnace, the method of metallurgical treatment, and the casting process itself.

For engineers, it is essential to know the expected properties of the selected material (such as hardness, strength, etc.) when designing a casting. While the mechanical properties of most commonly used materials have already been determined, these values are typically general and approximate. In real-world conditions, material properties may vary due to specific processing and operational factors. Therefore, it is crucial to verify these properties through material testing in accordance with established standards. These processes are crucial for reducing potential defects and ensuring the long-term reliability of the component. [8] [9]

In this article, the term 'Influence of Thermal Conditions' refers specifically to the combined effect of mould preheating temperature and pouring temperature on the solidification behaviour and resulting properties of the AlSi10Mg alloy. These thermal parameters determine cooling rates within the plaster-based investment mould and therefore directly influence microstructure formation, fluidity, thermal expansion, and mechanical performance.

2. Experiment description

The aim of the experiment was to evaluate the suitability of the given melt and mould temperatures in terms of fluidity, microstructure quality, linear thermal expansion, and tensile and compressive strength.

For this purpose, test castings were prepared according to a custom-designed model based on the spiral fluidity test [10], with emphasis on understanding the intended application of the final casting, as well as the shapes and processes used for its production. [11] The model consisted of a circular base with ten rods arranged around the perimeter, with diameters of 2; 2.5; 3; 3.5; 4; 5; 6; 8; and 10 mm. First, wax model components were produced using a LOGIMEC 2500 D wax injector under elevated pressure. These components were then assembled, placed in a flask. The gating system was designed for practical experimental purposes rather than metallostatic optimisation. Short gates with bottom-to-top filling were used, and the rods were open to air to prevent gas entrapment. The system size was limited by the crucible and furnace capacity, so metallostatic pressure was not a factor.

A quantity of 3,300 g of SRS Eurovest plaster was calculated and using a CIMO 92-4 plaster mixer the plaster was mixed with water. The water-to-powder ratio was 38 %, since our work did not involve producing artistic castings, and it was not necessary to achieve an exceptionally smooth surface. The mixture was mixed and subsequently poured into the flask under vacuum and after most of the flask volume was filled, vibration was used to ensure the maximum removal of air bubbles in the mould.

The invested wax patterns were removed from the plaster in a Memmert drying oven. The heating process was slow and gradual, increasing from 80 °C to 150 °C. This gradual temperature rise, as opposed to standard procedures involving rapid heating, ensured more controlled and uniform heating of the moulds. It allowed them to warm up evenly without major thermal shocks that could cause defects in the mould and, consequently, in the final casting. Once all the wax had been removed, the moulds were taken out of the furnace and allowed to cool in air.

The prepared moulds were then fired to remove all bound water. This was carried out in a KITTEC firing furnace, and the sequence of the entire firing process is shown in Fig. 1.

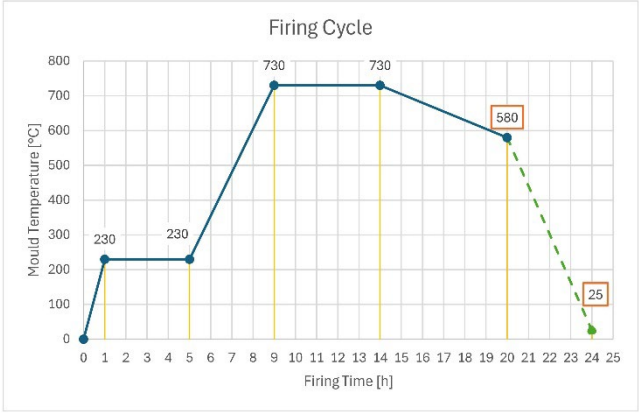

Fig. 1 Graph of the Firing Cycle

Once the moulds were properly prepared, test castings were poured from ingots of EN AC–AlSi10Mg alloy in accordance with ČSN EN 1706, the standard for aluminium casting alloys. The EN AC–AlSi10Mg alloy was selected because it offers excellent fluidity, good castability, and the ability to fill thin-walled, detailed, and complex shapes, making it particularly suitable for art castings produced by investment casting. Although this alloy is

commonly cast in ceramic shell moulds [1], there is limited research on its behaviour in plaster-based investment flask casting. Using this material therefore helps to address a knowledge gap regarding the performance of AlSi10Mg in plaster flask moulds compared to conventional ceramic shell moulds.

Melting was carried out in an electric resistance chamber furnace (LAC) using a graphite–chamotte crucible. No refining or degassing procedures were applied, and the hydrogen content of the melt was not measured. Gravity casting without vacuum was used as the casting technique. The furnace temperature was set to 750 °C. After removing the crucible, the melt temperature was measured using a thermocouple thermometer and allowed to decrease to 730 °C. The moulds, removed from the firing furnace at 580 °C, were measured using a standard thermometer and then cast. The melt temperature was subsequently allowed to drop further to 680 °C, where the next set of castings were cast.

Due to the size limitations of the crucible and furnace, the melting and casting process was carried out in batches of six moulds at a time. In total, 18 moulds were cast across three successive melts, with each batch of six moulds using a single melt.

The extreme mould temperatures of 25 °C and 580 °C were selected to investigate the influence of the lowest and highest possible mould preheating conditions on the microstructure and properties of the AlSi10Mg alloy. The maximum mould temperature of 580 °C was chosen because it approximates the liquidus temperature of AlSi10Mg, based on an average of experimental data from thermal analysis [12] and values from material property tables [13]. After casting at high temperature, moulds intended for the 25 °C condition were removed from the furnace and allowed to cool naturally in air to the desired temperature in a dry environment. The final temperature of 25 °C was verified using a standard thermometer, after which the casting was performed. While the risk of moisture uptake by the moulds prior to casting could not be entirely excluded, no obvious signs of gas porosity attributed to moisture were observed in the microstructures, although, this was not specifically measured.

Six different casting conditions were applied, and one of the resulting test castings is shown in Fig. 2.

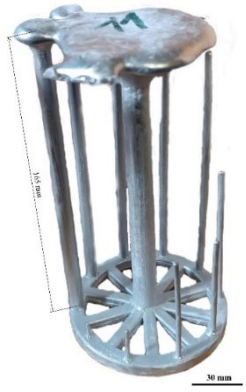

Fig. 2. Test Casting

Before sectioning the castings and preparing the test specimens for material analysis, fluidity measurements were recorded. In this study, the term ‘fluidity’ refers specifically to alloy fluidity. Fluidity was assessed using a stepped rod test mould with a total channel length of 165 mm. This length corresponds to the length of the original wax model used to prepare the investment mould and was therefore taken as the reference value representing 100 % alloy fluidity. Subsequently, metallographic examinations, linear thermal expansion tests, and tensile and compressive strength tests were conducted.

2.1. Testing of Samples

For the determination of linear thermal expansion, test specimens were prepared from rods with a diameter of 6 mm and a length of 25 mm. Measurements were conducted using a Netzsch DIL 402 C dilatometer in a horizontal configuration under an inert argon atmosphere.

Metallographic examinations were carried out on samples with diameters of 2 mm, 6 mm, and 10 mm. The ground, polished, and etched specimens were analysed using an optical microscope. Microstructural images were recorded at magnifications of 25× and 100×, with 100× magnification used for comparative analysis of the results.

Tensile test specimens were machined directly from cast rods with an initial diameter of 8 mm and a total length of 130 mm. The rods were produced as part of the experimental casting trials, and therefore the tensile geometry did not follow any specific standard. Instead, the available rod dimensions were used intentionally in order to evaluate the mechanical behaviour of the as-cast material under minimal machining. The gauge region of the specimens was left exactly in the as-cast condition, without introducing a notch or fillet radius. This approach was chosen deliberately to allow the tensile test to reflect the true casting quality, including surface condition, local defects, grain refinement, and feeding quality.

Such samples were subjected to tensile testing on a ZWICK/ROELL Z150 testing machine, where they were exposed to tensile stress until fracture.

Compressive test specimens were cylindrical samples with a diameter of 10 mm and a height of 15 mm, prepared for uniaxial compression testing. These samples were tested using a Gleeble 3800 GTC thermomechanical testing system equipped with the Hydrawedge II testing module.

The dimensions of all specimen types used for individual tests are shown in Fig. 3.

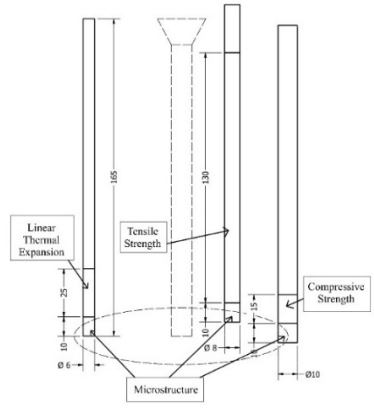

Fig. 3 Diagram of sections for the individual specimens

3. Discussion of Results

Based on the obtained test data, an analysis was conducted to evaluate the impact of individual parameters on material quality and behaviour.

3.1. Fluidity

The fluidity measurement was not performed according to a specific standard. Instead, an individual experimental method, based on the Czikela method, was used, and adapted to the conditions of casting into plaster flask moulds. This approach was chosen because conventional standardised fluidity tests are typically designed for sand moulds or metal moulds and are not directly applicable to plaster-based investment casting. Our method relies on determining the distance that the molten metal is able to flow within vertically arranged test rods of circular cross-section. First, a model was designed in a 3D CAD program and subsequently produced using a 3D printer. Silicone moulds were then created from these models to enable repeated production of wax patterns for the investment casting process.

A general assessment of fluidity indicates that the pouring temperature alone did not significantly affect the fluidity of the metal compared to the increase in mould temperature. Compared to moulds at 25 °C, the flow length significantly improved when the moulds were preheated to 580 °C. At identical pouring temperatures, increasing the mould temperature resulted in fluidity increases of 14 %, 28 %, and 42 %, respectively, for the three castings tested.

In the first graph (Fig. 4), which represents the relationship between pouring temperature and fluidity for moulds at 25 °C, significant changes in fluidity can be observed, showing a clear trend of decreasing fluidity with a decrease in pouring temperature. In contrast, in the second graph (Fig. 5), which illustrates the fluidity behaviour of castings poured into moulds preheated to 580 °C, this effect is diminished, and the variations depending on pouring temperature are minimal.

The fluidity of the alloy presented in Figs. 4 and 5 shows the average values representing the arithmetic mean of three separate castings produced under each casting condition. For each parameter, three series were prepared to minimise deviations. An overall mean for each casting condition is also indicated at the bottom of the graphs to provide an overview of the alloy's behaviour.

Given the rod diameters, fully flowed rods are observed only at larger diameters at lower temperatures, while at higher temperatures (both mould and pouring temperatures), the overall fluidity values are higher even for smaller diameters. When comparing the total flow distance, it can be concluded that the increased mould temperature has a far more significant effect on fluidity than the increased pouring temperature. This is demonstrated, for instance, by comparing the flow percentages of rods with the same diameter and pouring temperature, visible at Fig. 4 and 5.

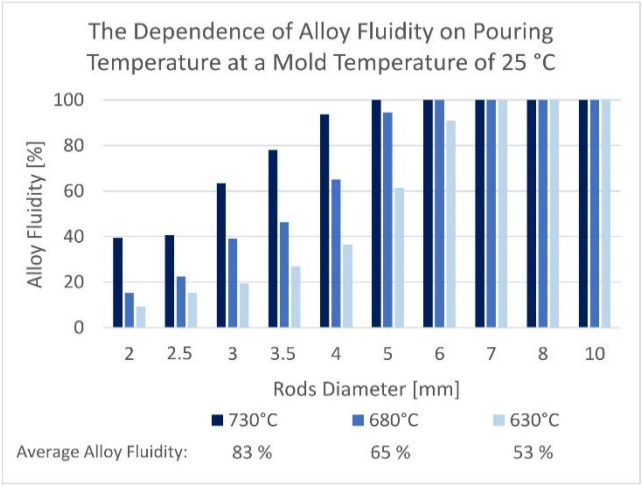

Fig. 4. Graph of the dependence of alloy fluidity on pouring temperature at a mould temperature of 25 °C

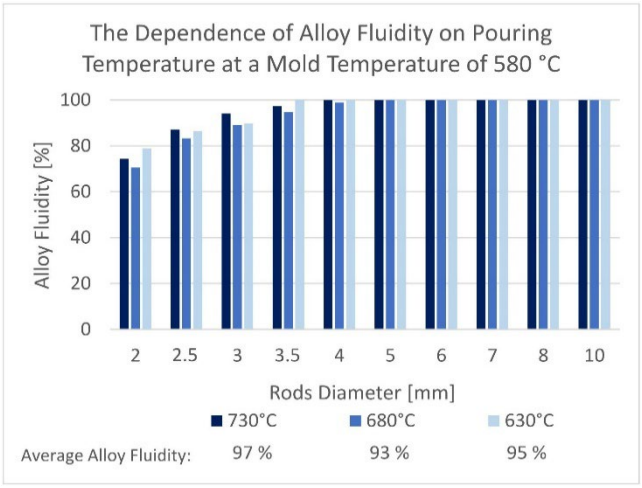

Fig. 5. Graph of the dependence of alloy fluidity on pouring temperature at a mould temperature of 580 °C

3.2. Microstructure

When comparing the microstructure, a typical trend can be observed: with longer solidification times caused by higher mould temperatures, the structure is less fine-grained (Fig. 7, 9, 11, 14, 15) than in cases of rapid cooling. At room temperature moulds of 25 °C (Fig. 6, 8, 10, 12, 13), the material exhibits a significantly finer grain structure and a lower number and size of shrinkage cavities, which are caused by the volume contraction of the metal during solidification. The microstructural images clearly reveal the α Al phase (white areas) and the eutectic phase (black needles) formed by silicon. Based on their shape, it can be identified as a eutectic with a lamellar structure.

Regarding porosity, castings poured at higher temperatures exhibited the most unfavourable properties, particularly in Fig. 11, 14, and 15, where large and numerous shrinkage defects are visible. The finest grained structure can be clearly observed in the casting

with the smallest diameter of 2 mm, poured at the lowest pouring temperature of 630 °C into a mould at 25 °C.

Significant differences were observed between the microstructural changes at a constant pouring temperature while varying the mould temperature from 25 °C to 580 °C. The comparison is shown in Fig. 6–11, where the microstructures of castings poured at the same temperature into rods of identical diameters (2, 6, and 10 mm) are displayed side by side. A substantial refinement in grain structure and the occurrence of shrinkage defects confirms the dominant influence of mould temperature on microstructural quality. In the following four images (Fig. 12, 13, 14, 15), it can be observed that castings poured at different pouring temperatures (630 °C and 730 °C) into moulds at the same temperature exhibit minimal microstructural differences. This further supports the assertion that mould temperature changes have a greater impact than variations in pouring temperature.

Eutectic silicon with an elongated needle-like shape is considered one of the factors contributing to lower mechanical properties, as it is assumed to act as an obstacle to dislocation movement, which acts as stress concentrators, leading to premature failure. During mechanical loading, these castings tend to fracture more rapidly, and tensile strength tests confirm that they exhibit lower ultimate tensile strength values. [14]

For grain refinement evaluation, secondary dendrite arm spacing (SDAS) and the percentage of eutectic silicon phase were manually determined from microstructural images. The measurements of SDAS and eutectic phase percentage, were performed on samples taken from cast rods with a diameter of 6 mm. This diameter was selected because the same rod geometry was also used for the linear thermal expansion tests, ensuring that both microstructural and dilatometric data originate from castings solidified under identical thermal conditions. This helps eliminate variability caused by different cooling rates and enables a more direct comparison between microstructure, thermal behaviour, and mechanical response.

The SDAS values were measured using the method described in [15], which involves measuring the primary dendrite arm spacing and counting the secondary dendrite arms on both sides of the primary arm. The distances were measured in four different directions using Quick-PHOTO INDUSTRIAL 3.2 software, and the final value was determined as the average. The results showed a clear trend: lower SDAS values are associated with higher mechanical properties due to the formation of a finer solidification phase. The average SDAS values for castings poured into room-temperature moulds (25 °C) ranged from 25 to 28 µm, while castings poured into preheated moulds at 580 °C had values ranging from 67 to 70 µm. These measurements were performed on castings with a 6 mm diameter, which were also subjected to thermal expansion tests. The general rule that a reduction in SDAS leads to improved homogeneity and enhanced mechanical properties due to the refinement of the solidification phase was confirmed, highlighting the importance of rapid solidification in ensuring high-quality material.

By utilizing the previously mentioned software for processing microscopic image documentation, the percentage of the eutectic silicon phase was determined from the same samples used for SDAS measurements. The values are presented in Table 1, where the samples with the highest ultimate tensile strength are highlighted in green, while those with the lowest are marked in red.

Table 1.
Microstructure values of the samples

t_{mould} [°C]	$t_{pouring}$ [°C]	Eutectic Si phase [%]	SDAS [µm]
25	**630**	19,02	25,01
25	**680**	19,28	26,31
25	**730**	19,96	27,75
580	**630**	12,11	67,35
580	**680**	13,05	69,93
580	**730**	11,76	68,82

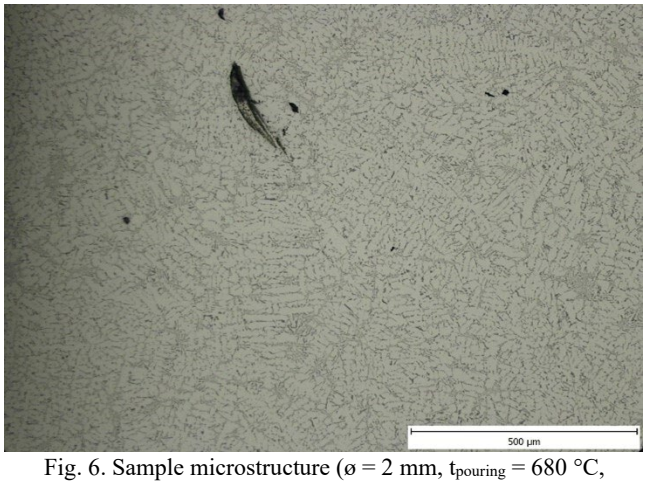

Fig. 6. Sample microstructure (ø = 2 mm, $t_{pouring}$ = 680 °C, t_{mould} = 25 °C)

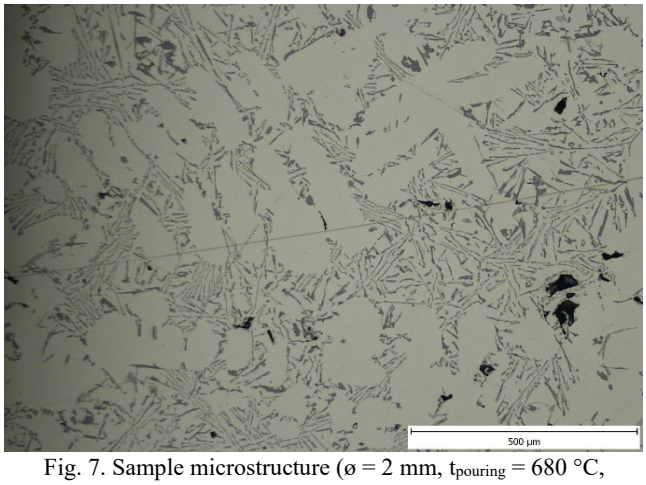

Fig. 7. Sample microstructure (ø = 2 mm, $t_{pouring}$ = 680 °C, t_{mould} = 580 °C)

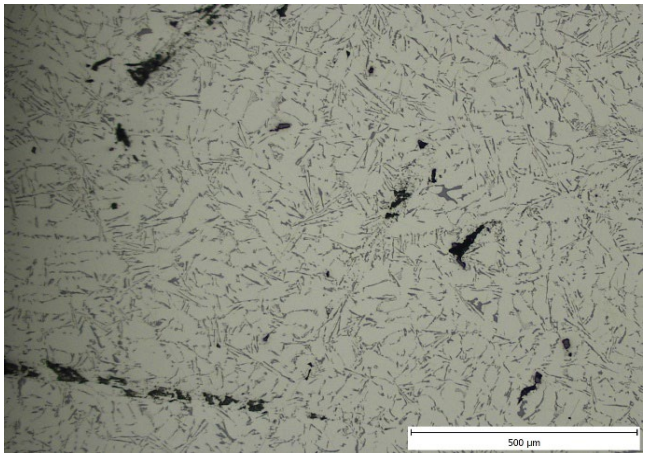

Fig. 8. Sample microstructure (ø = 6 mm, $t_{pouring}$ = 680 °C, t_{mould} = 25 °C)

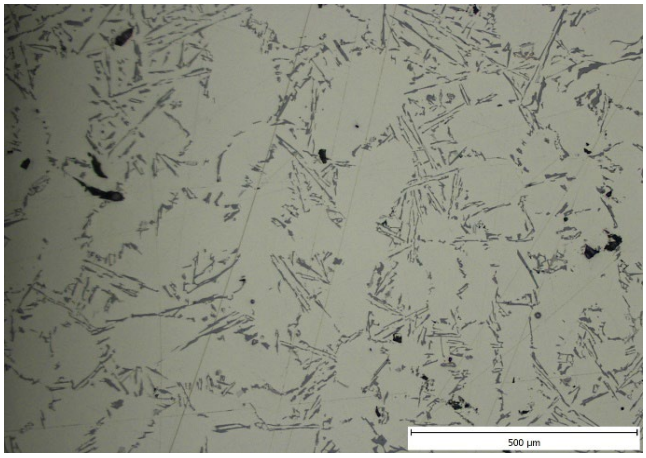

Fig. 9. Sample microstructure (ø = 6 mm, $t_{pouring}$ = 680 °C, t_{mould} = 580 °C)

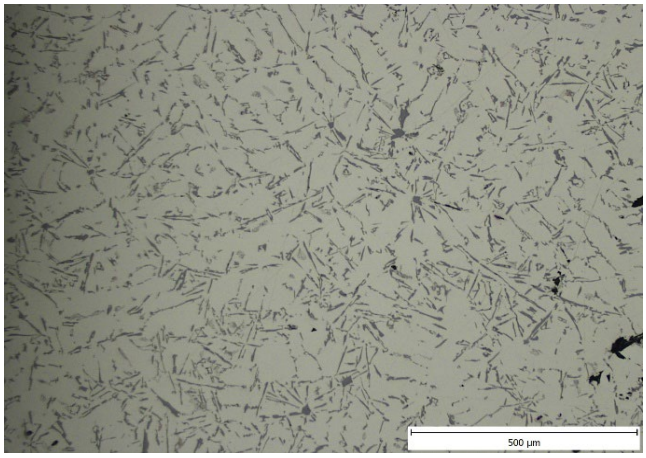

Fig. 10. Sample microstructure (ø = 10 mm, $t_{pouring}$ = 680 °C, t_{mould} = 25 °C)

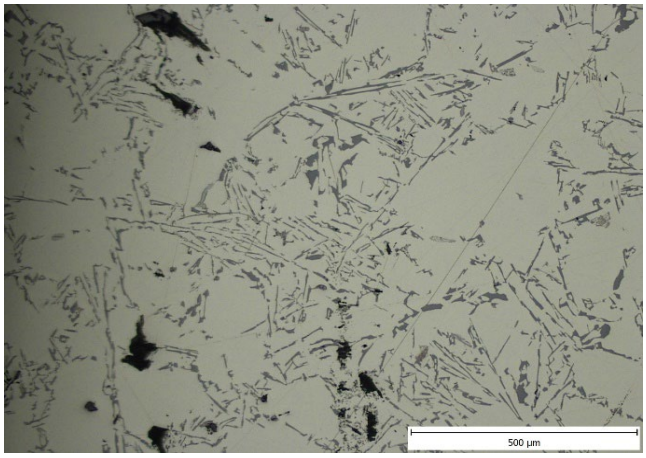

Fig. 11. Sample microstructure (ø = 10 mm, $t_{pouring}$ = 680 °C, t_{mould} = 580 °C)

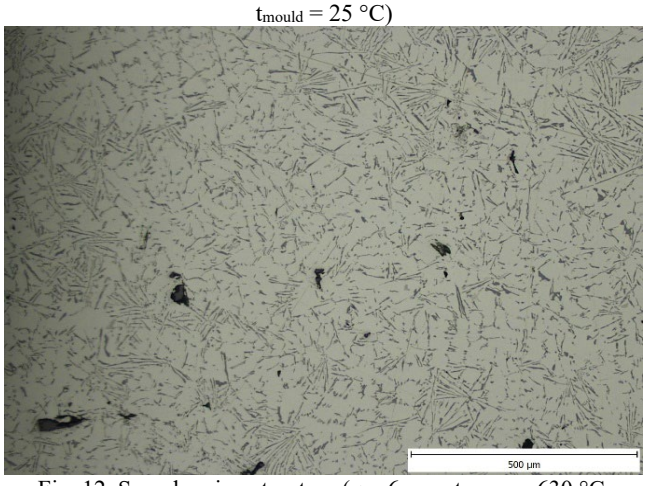

Fig. 12. Sample microstructure (ø = 6 mm, $t_{pouring}$ = 630 °C, t_{mould} = 25 °C)

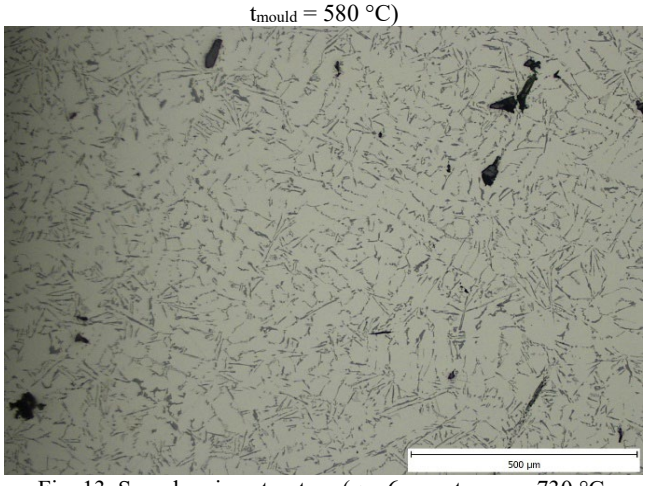

Fig. 13. Sample microstructure (ø = 6 mm, $t_{pouring}$ = 730 °C, t_{mould} = 25 °C)

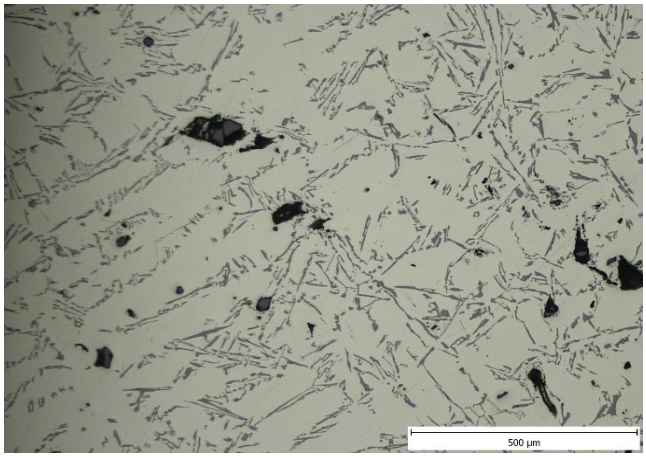

Fig. 14. Sample microstructure (ø = 6 mm, $t_{pouring}$ = 630 °C, t_{mould} = 580 °C)

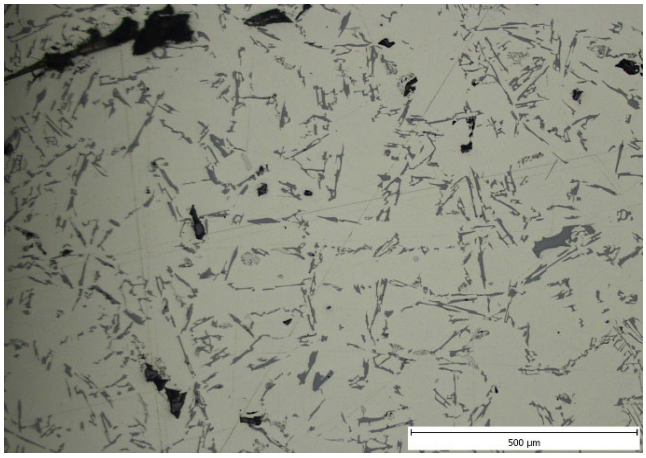

Fig. 15. Sample microstructure (ø = 6 mm, $t_{pouring}$ = 730 °C, t_{mould} = 580 °C)

Here, we can observe that castings that cool rapidly and are poured into cooler moulds exhibit a higher proportion of eutectic compared to castings poured into moulds preheated to 580 °C. In their microstructure, there are larger dendrites, providing more space for the primary aluminium phase. These results again confirm the previously established claims. Higher cooling rates result in a finer-grained structure with a higher proportion of eutectic, a factor contributing to achieving higher mechanical properties in the final material.

From a microstructural perspective, individual samples poured under the same temperatures and conditions but with rods of different diameters can also be compared. The comparison was made with the rod of the smallest diameter of 2 mm, with a diameter of 6 mm, and with the rod of the largest diameter of 10 mm. This confirmed the expected trend of increased fineness and reduced size and number of shrinkage porosity and shrinkage cavities with decreasing rod diameter. The microstructure of the narrowest rod, cast at the lowest pouring temperatures into an unpreheated mould, achieved an SDAS of 10.32 µm and the highest proportion of eutectic at 30.63 %, which was the highest value among all castings. It can therefore be stated that the highest mechanical values would be achieved by castings poured into narrow diameters with fast cooling ensured by the mould temperature of 25 °C. However, with the same rod diameter, but poured at the highest pouring temperature of 730 °C into a mould preheated to 580 °C, a lower eutectic proportion of 12.48 % and an increased SDAS value of 32.01 µm were measured. When comparing rods with the largest diameter of 10 mm, the least favourable results were obtained in terms of expected low mechanical properties. At the lowest pouring and mould temperatures, the eutectic proportion was 17.85 % and SDAS was 42.42 µm. When poured at the highest pouring temperature into preheated moulds, the values compared to all other measurements were the least suitable for material use. Here, SDAS reached up to 92.39 µm, and the eutectic proportion was 11.52 %. The average values of the changes in the parameters described above, measured on 6 mm diameter rods, are graphically displayed in the charts in Fig. 16 and 17. These figures also reflect the expected measurement uncertainty, as the presented values are averages and no error bars are shown. The differences between the pouring temperatures of 630, 680 and 730 °C are relatively small and may therefore fall within the measurement error. In these graphs, the main intention is to highlight the significant contrast between the samples cast into a mould at 25 °C and those cast into a mould preheated to 580 °C, rather than to emphasise minor variations among the individual pouring temperatures.

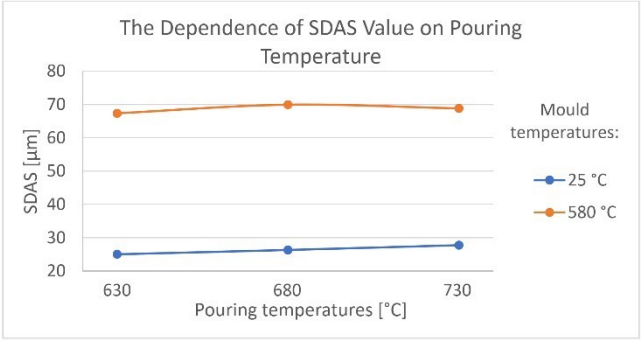

Fig. 16. Graph of the dependence of SDAS value on pouring temperature

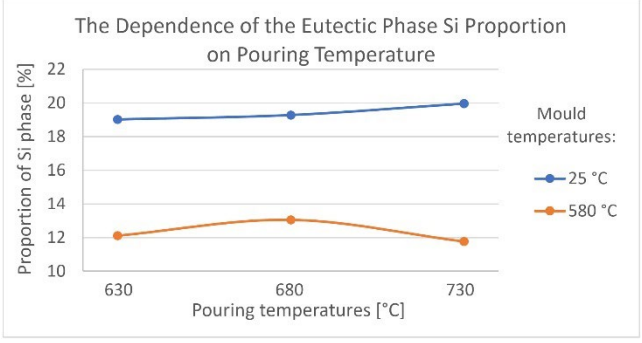

Fig. 17. Graph of the dependence of the proportion of the eutectic Si phase on pouring temperature

3.3. Linear Thermal Expansion

In evaluating linear thermal expansion, it can be observed that utilizing higher mould temperatures is more advantageous. This results in slower cooling and dendrite growth, leading to internal porosity or shrinkage. The comparison of the expansion behaviour for the given mould temperature is shown in the graphs in Fig. 18 and 19, with the final overall expansion of the sample in percentage, measured at 553 °C, compared in Table 2. The curve for the 730 °C pouring temperature is not separately visible in Fig. 19 because it closely overlaps with the curve for 680 °C, following the same trend. In both graphs, only visible and relevant error bars are shown, while those with a standard deviation below 0.3 % of the original measured value are omitted.

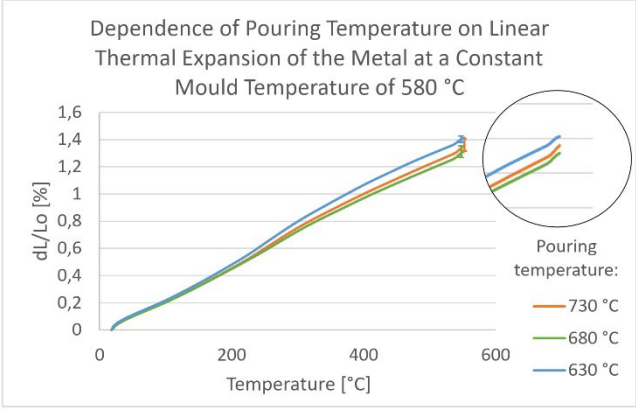

Fig. 18. Graph of the dependence of pouring temperature on the linear thermal expansion of the metal at a constant mould temperature of 580 °C

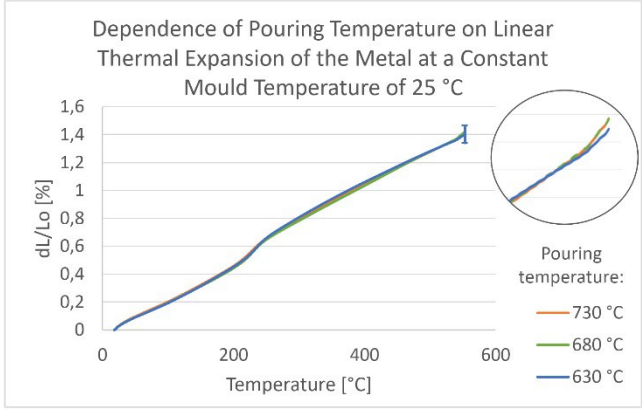

Fig. 19. Graph of the dependence of pouring temperature on the linear thermal expansion of the metal at a constant mould temperature of 25 °C

Table 2.
Values of linear thermal expansion

Order of expansion (from lowest)	Pouring temperature [°C]	Mould temperature [°C]	Values of thermal expansion [%]
1.	680	580	1.315
2.	730	580	1.360
3.	630	25	1.403
4.	630	580	1.412
5.	680	25	1.421
6.	730	25	1.423

According to general assumptions and practical tests conducted by the authors [16], the values of linear thermal expansion are expected to increase with an increasing mould temperature, or with a slower cooling rate of the casting. However, the measured values did not confirm this phenomenon, which may be attributed to several factors. One possibility is the amount and morphology of the silicon eutectic, which can, in some cases, influence linear thermal expansion and lead to its increase. Another potential explanation lies in the differing thermal properties of the primary aluminium phase and the eutectic, or their interactions. The differing thermal expansions and distinct behaviours of these individual phases may also explain the observed increase in linear thermal expansion. From a microstructural perspective, the absence of metal volume in areas of shrinkage and porosity might contribute to the relaxation of expansion in individual grains of the material. This could counteract the negative effects of air trapped in these cavities within the casting. In terms of grain size, another possible explanation could involve the quantity of individual grains. In a finer-grain structure, there are more individual particles, each of which micro-expands separately at elevated temperatures. These individual micro-expansions accumulate, causing the resulting macro-expansion to potentially exceed that of a coarser-grained structure. In this case, while the individual grains are larger and expand more, their smaller number leads to a lower overall linear thermal expansion.

3.4. Tensile and Compressive Strength

The tensile behaviour of the alloy shows a clear dependence on the cooling rate determined by the mould temperature. Faster cooling in cold moulds (25 °C) produced finer-grained microstructures with reduced porosity, leading to improved mechanical performance.

Ultimate tensile strength (R_m) reached 154 to 168 MPa for samples cast in 25 °C moulds, compared with only 123 to 136 MPa for samples cast in preheated moulds at 580 °C. This represents an increase of up to 26.8 %. The highest strength of 167 MPa was in combination with a pouring temperature of 730 °C.

Yield strength ($R_{p0.2}$) exhibited the same trend. Cold-mould samples reached 96 to 107 MPa, while preheated-mould samples showed only 80 to 85 MPa, a reduction of nearly 25 % strength due to slower solidification and greater pore formation.

The elastic modulus (E) varied from 51 to 62 GPa, with no strict monotonic trend. The scatter likely reflects differences in local micro-defects and the as-cast testing surface.

The elongation to fracture (Z) also correlates strongly with cooling rate. Samples from cold moulds achieved 3–5 %, whereas preheated mould samples reached only 1–2 %, a reduction of up to 70 %. This confirms that porosity formation at slower cooling severely limits ductility.

These results show that rapid cooling in unheated moulds not only increases strength, but also preserves ductility, which is an important combination for small cast components.

The rapid cooling also influenced contraction, which was higher (up to 5 %) in fast-cooled castings compared to slowly cooled ones (as low as 1 %). In relative terms, this is an increase of up to 80 %.

A compressive strength test was performed on the rods because they were prepared primarily as standard specimens to evaluate casting properties such as fluidity. Even though the rods are long and thin, compressive strength testing is straightforward and provides basic information on material integrity and defect presence, which is useful for quality control during casting trials.

In real service, the final cast products intended to be created by the method researched in this study are small decorative or artistic pieces, that would mainly experience compressive loads rather than bending. Therefore, compressive testing of the rods adequately reflects the mechanical reliability of the material. A flexural test, while possible, would not significantly improve the assessment for these intended applications.

Compressive strength results follow a similar trend. Samples cast into 25 °C moulds reached compressive strengths of 210 to 225 MPa, while those cast into preheated moulds (580 °C) achieved only 170 to 180 MPa. All tested samples showed typical behaviour – rapid strain hardening followed by stable plastic flow, where strain hardening and material recovery balanced out. Faster-cooled samples again showed better mechanical resistance, confirming that finer grain structures improve overall mechanical performance. The overall progressions of the individual tests are shown in the curves presented in Fig. 20 and Fig. 21.

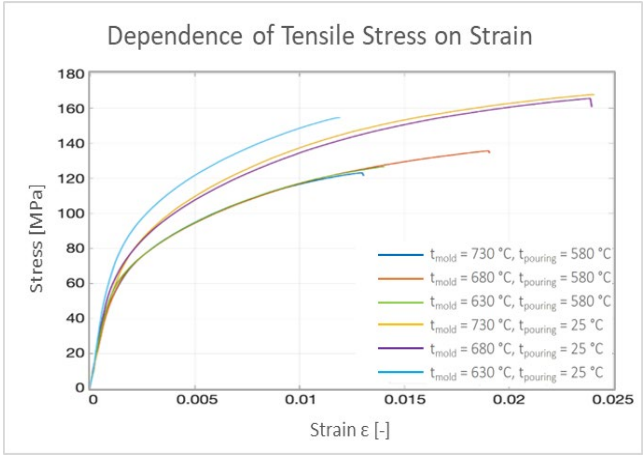

Fig. 20. Graph of the dependence of tensile stress on strain

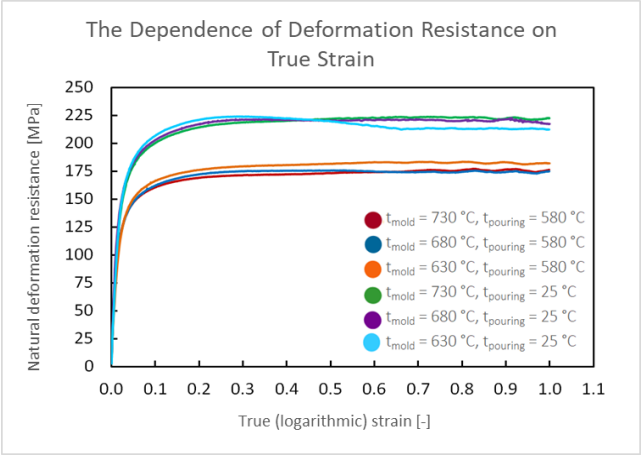

Fig. 21. Graph of dependence of deformation resistance on true strain

3.5. Final Comparison

For the final comparison, samples representing the highest quality in each measured area are presented.

The optimal casting conditions in terms of linear thermal expansion were a pouring temperature of 680 °C and a mould temperature of 580 °C. In this case, the total expansion was the lowest at 1.32 %, the structure was coarser-grained, but there was no significant presence of porosity or shrinkage cavities. Fluidity was high, even for rods with smaller diameters.

From a microstructural perspective, the most favourable conditions were a pouring temperature of 630 °C and a mould temperature of 25 °C. The resulting microstructure was the finest-grained, but the expansion was higher at 1.40 %, and the fluidity was the lowest. The smallest rod diameter of 2 mm had a fluidity value below 10 %. For casting complex and thin-walled components, such low fluidity would be a significant issue and would most likely prevent the production of a high-quality, defect-free casting. The mechanical properties under these conditions were very favourable; however, both fluidity and linear thermal expansion were inadequate.

The most suitable casting conditions for achieving the highest fluidity, with an overall value of up to 97 %, were obtained at the highest pouring temperatures – 730 °C and a mould temperature of 580 °C. The linear thermal expansion was the second lowest at 1.36 %. However, the microstructure was very coarse-grained and contained a significant amount of porosity and shrinkage cavities, caused by the high temperature and low cooling rate.

4. Conclusion

The aim of this research was to describe the behaviour of the AlSi10Mg alloy cast under various solidification and casting conditions. Based on the obtained results of material testing—such as fluidity, microstructure evaluation, linear thermal expansion at elevated temperatures, and tensile and compressive strengths—it was possible to identify how casting parameters affect the material

properties and to define favourable ranges for these parameters. The objective was to understand the conditions that ensure a high-quality material with sufficient performance across all investigated parameters.

Lower mould temperatures (25 °C in this study) were found to be more beneficial for improving material properties, as higher mould temperatures led to a deterioration in the mechanical performance of the alloy. The pouring temperature could be adjusted to compensate for the reduced fluidity caused by the low mould temperature, making 680 °C or 730 °C more suitable choices. However, an increase in pouring temperature also results in an undesired rise in linear thermal expansion, though this effect is offset by the improvement in mechanical properties in the overall assessment.

Extreme mould temperatures of 25 °C and 580 °C were used to explore the limits of the process, and significant differences were observed in the measured properties. While the high temperature of 580 °C was intentionally chosen to examine the upper thermal limit, for more practical applications it is advisable to preheat moulds to intermediate temperatures (e.g., 300–430 °C). This approach reduces extreme variations in material properties and allows the alloy to be used in a broader range of applications.

Acknowledgment

This research has been supported by project SP 2025/026 („Research and application of non-traditional sources of secondary raw materials“) of the Ministry of Education, Youth and Sports and realized within the framework of the Technology Agency of the Czech Republic project SIGMA DC2 nr. TQ15000341. Additionally, the infrastructure used was made available through project of MEYS (grant number CZ.02.1.01/0.0/0.0/17_049/0008399).

References

[1] Beeley, P. (2001). *Foundry Technology* (2nd ed.). Retrieved 6 March 2025, from https://www.academia.edu/4161769/foundry_technology_by_peter_beeley. DOI: 10.1016/B978-0-7506-4567-6.X5000-6.

[2] Raj, R.J., Panneer Selvam, P. & Pughalendi, M. (2021). A review of aluminum alloys in aircraft and aerospace industry. *Journal of Huazhong University of Science and Technology.* 50(4). ISSN-1671-4512

[3] Ashkenazi, D. (2019). How aluminum changed the world: A metallurgical revolution through technological and cultural perspectives. *Technological Forecasting and Social Change*. 143, 101-113. DOI: 10.1016/j.techfore.2019.03.011.

[4] Yoshida, H. (2023). History of the development of extra super duralumin and future research issues of Al–Zn–Mg alloys. *Materials Transactions*. 64(2), 341-351. DOI: 10.2320/matertrans.MT-LA2022019.

[5] Hampl, J. (2014). *Metalurgie slévárenských slitin: studijní opora*. Ostrava: VŠB – Technická univerzita Ostrava. ISBN 978-80-248-3585-3

[6] Pian, W., Zhou, Y., Xiao, T. (2023). A review of the feasibility of aluminum alloys, carbon fiber composites and glass fiber composites for vehicle weight reduction in the automotive industry. *Journal of Physics: Conference Series*. 2608, 012005, 1-10. DOI: 10.1088/1742-6596/2608/1/012005.

[7] Duclos, A., Bernardi, E., Robbiola, L., Deshayes, C., de Souza Machado, L., Martini, C., Chiavari, C., Balbo, A., Escobar, C., Guilmionot, E., Malard, B. & Brunet, M. (2024). Duralumin alloys in World War II heritage aircraft: Correlations between manufacturing parameters and alloys' properties. *Heritage*. 7(12), 6772-6790. DOI: 10.3390/heritage7120313

[8] Luo, A. A., Sachdev, A. K. & Apelian, D. (2022). Alloy development and process innovations for light metals casting. *Journal of Materials Processing Technology.* 306, 117606, 1-28. https://doi.org/10.1016/j.jmatprotec.2022.117606.

[9] Roučka, J. (2004). *Metalurgie neželezných slitin*. Brno: Akademické nakladatelství CERM. ISBN 80-214-2790-6

[10] Futáš, P., Petrík, J., Pribulová, A. (2014). The analysis of Al-Si alloy fluidity test in computer simulation. In Proceedings of the 14th SGEM GeoConference on Informatics, Geoinformatics and Remote Sensing, 17-26 June 2014 (pp. 45-50). DOI: 10.4028/www.scientific.net/KEM.635.45

[11] Çolak, M. & Yalçın, Ö. (2025). Investigation of the effect of niobium addition on fluidity and mechanical properties in casting of aluminum alloys. *International Journal of Metalcasting*. 20, 473-481. DOI: 10.1007/s40962-025-01613-8.

[12] Vončina, M., Mrvar, P., Medved, J. (2005). *Thermodynamic analysis of AlSi10Mg alloy*. Retrieved December 2, 2025, from http://www.dlib.si/URN:NBN:SI:DOC-3XZIBUAR

[13] Pin Manufacturing Company. (2024). *Alloy data*. Retrieved 2 December 2025, from https://pinmfgco.com/wp-content/uploads/2024/01/Alloy-Data.pdf

[14] Zýka, J. (2016). *Influence of microstructure on mechanical properties of MAR-M-247 nickel superalloys*. Retrieved from https://issuu.com/inasport/docs/slevarenstvi_rocnik_lxiv_2016_11_12

[15] Vandersluis, E. & Ravindran, C.R. (2017). Comparison of measurement methods for secondary dendrite arm spacing. *Metallography, Microstructure, and Analysis*. 6(1), 89-94. DOI: 10.1007/s13632-016-0331-8.

[16] Radkovský, F., Gawronová, M., Válková, N., Lichý, P., Kroupová, I., Merta, V. & Nguyenová, I. (2022). Determination of linear expansion of AlSi10Mg aluminium alloy depending on external conditions during solidification. *Heliyon*. 8(11), 1-10. DOI: 10.1016/j.heliyon.2022.e11363